JOURNAL OF SPACECRAFT AND ROCKETS
Vol. 31, No. 5, September–October 1994

Fourth-Generation Mars Vehicle Concepts

Brent Sherwood*
Boeing Defense & Space Group, Huntsville, Alabama 35824

Conceptual designs for crew-carrying Mars transfer and excursion vehicles, fully integrated to state-of-the-art standards, are presented. Developed since 1990 under contract to NASA, these concepts incorporate improved understanding in many key fields and take full advantage of advanced computer-based analysis and design methodologies. The three generations of Mars vehicle design concepts that evolved from 1952 to 1990 are briefly reviewed. Fourth-generation requirements, constraints, and options for manned Mars missions in the early decades of the 21st century are then summarized. The resulting vehicle concepts are sized for six crew members, and can support all opposition and conjunction opportunities in or after 2014. The modular, reusable transfer ship is launched to Earth orbit on six 185 tonne-class boosters and assembled there robotically. Its dual nuclear-thermal rocket engines use liquid hydrogen propellant. The payload consists of a microgravity habitation system and an expendable lift-to-drag = 1.6 lander capable of aeromaneuvering to sites within ±20 deg of the equator. This lander can deliver either an expendable, storable-bipropellant crew-carrying ascent vehicle, or 40 tonnes of cargo, and it is capable of limited surface mobility to support base buildup. Multiple cargo landers sent ahead on robotic transfer vehicles deliver the supplies and equipment required for long-duration surface missions.

Introduction

THE first-generation technical analysis of human missions to Mars was published four decades ago.[1] Von Braun intended it as a proof-of-concept "to demonstrate that on the basis of the technologies and the know-how then available" human exploration of Mars was possible. Low-energy transfer constrained the concept to a conjunction-class (449-day) staytime at Mars. The supplies and the enormous amount of storable propellants needed for propulsive planetary capture required ten ships on the expedition, of which three landed with a total payload of 149 tons. The lack of automation technology led to a mission crew of 70 men. Forty-six shuttles flew 950 Earth-to-orbit (ETO) delivery flights in just eight months, consuming 10 times the fuel used for the Berlin airlift.

Exploration planners have been trying to reduce the scale of Mars missions since that time. The technological progress of the 1960s and 1970s enabled a second generation of Mars mission design to occur. Von Braun himself, buoyed by the success of the first human space flights, wrote in 1962 that new re-entry techniques would allow aerobraked Earth descent direct from hyperbolic speeds, thus saving enormous amounts of propellant. Furthermore, he invoked three new propulsion options capable of dramatically improving interplanetary transfer efficiency: a cryogenic chemical (LOX/hydrogen) option, a nuclear thermal (NTP) option, and a nuclear ion (NEP) option.[1] Von Braun favored NEP, but NTP went on to full-scale development testing through 1973, and it was the clear leader for Mars applications. Pulsed fission propulsion was also proposed (Orion),[2] making Mars seem merely the first stop for nuclear-powered space exploration.

Proposals for human deep-space exploration suffered neglect in the post-Apollo decade. In the 1980s, the third generation of Mars mission design began slowly as an outgrowth of studies for much more modest orbital transfer vehicle (OTV) missions to geosynchronous orbit. By then flight experience had made cryogenic propulsion the baseline, and aerobraking was widely considered as the enabler for return to low Earth orbit (LEO) because of its leverage on reducing vehicle initial mass (IMLEO). Extending aerobraking to planetary capture, and enlarging cryogenic propulsion systems for trans-Mars injection (TMI), seemed practical and led to a new Mars mission type. Concern about multiyear reliability favored opposition mission profiles with 30–60-day staytimes, and IMLEO sensitivity held crew size to four. Complex third-generation designs were developed to accommodate aerobraking, large-radius artificial gravity, partial reusability, and robotic space assembly.[3] These cryogenic-aerobraked (CAB) vehicles assembled in LEO drydock became the basis for NASA's 90-Day Study,[4] compiled in 1989 in response to the announcement of a Space Exploration Initiative (SEI) by President George Bush.

From 1990 until its end in 1992, SEI dramatically advanced the technical community's understanding in several key fields: space and Mars science, contextual mission analysis, advanced propulsion options (especially NTP), aeromaneuvering in the martian atmosphere, long-duration habitation system design, lander and surface mobility system configuration, flight operations, in-space assembly and processing, and Earth-to-orbit transportation. In particular, NASA's multiyear study contract, *Space Transfer Concepts and Analysis for Exploration Missions* (STCAEM, NAS8-37857), pioneered the integrated application of advanced computational tools—supercomputer flight dynamics calculations, automated radiation dose analysis, and computer-aided design (CAD) and drafting—to planetary exploration conceptual design.[5] This paper presents the resulting fourth-generation Mars mission vehicle designs.

Space Exploration Initiative Mars Mission Constraints

Top-level, fourth-generation requirements came from several sources. President Bush specified only that human missions to Mars should occur after some form of permanent return to the Moon, but before the year 2019. The Augustine Committee[6] recommended integrating human planetary exploration into a balanced "Mission from Planet Earth" program, with space science as its primary goal, using robotic and human technologies as equal partners. The committee also recommended not burdening Space Station Freedom with the mission of being an interplanetary transportation node.

The Synthesis Group[7] established several more specific guidelines. Mars mission hardware would be tested first on dedicated lunar missions. The first human Mars mission would be opposition-class, with short-transfer conjunction-class profiles for all subsequent missions. The first mission would occur as early as 2014, supported by robotic surface cargo delivery on the 2012 opportunity. Missions would be launched on every opportunity (every 26 months) indefinitely. NTP propulsion and microgravity transfer would be baselined. Crew size would be six. Vehicle assembly in LEO would be eliminated if possible, and simplified to a rendezvous-and-dock operation where required. Crew return would use direct entry, and the transfer vehicle would be expendable early in the program.

Presented as Paper 93-1069 at the AIAA/AHS/ASEE Aerospace Design Conference, Irvine, CA, Feb. 16–19, 1993; received May 28, 1993; revision received Nov. 2, 1993; accepted for publication Nov. 3, 1993.

*Senior Specialist Engineer, Advanced Civil Space Systems, Missiles & Space Division, JC-19, P.O. Box 240002. Member AIAA.

To support NASA's input to the Synthesis process, STCAEM had already developed comparable concepts for the five primary Mars transfer propulsion options.[8] Based on that work, the study had recommended NTP, minimum crew size of six, a three-burn TMI (to enlarge the departure window), elliptical parking orbits at Mars (to minimize IMLEO) and moderately high lift-to-drag (L/D) ratios for Mars landers (to improve cross-range, controllability and heating). Independent analysis[9] subsequently suggested that the kind of science activities allowed by repeated, multiyear surface stays called for global access at Mars and more generous payload mass allowances than typically assumed.

Post-Synthesis, STCAEM went on to develop an integrated NTP vehicle concept responsive to all these requirements.[10] For the transfer vehicle, IMLEO was relegated as secondary to design simplicity. Specific design criteria were the following: integration of subsystem constraints; accommodation of any lander vehicle geometry, with shirtsleeve access from a transfer habitat module designed for microgravity; configured use of onboard resources for radiation protection; commonality in the dimensions of tanks and other structures; complexity-avoidance in LEO assembly operations; and ETO delivery by a minimal number of 150 tonne-class launches using a 12×32 m shroud. For the reference lander, a high-L/D design (HMEV) was developed to the same level of detail as the low- and moderate-L/D designs produced earlier by STCAEM. Specific lander design criteria were the following: use of an expendable $L/D \sim 1.6$ aerobrake; unmanned delivery of large-volume and mixed-manifest cargo, or delivery of a storable-propellant crew ascent vehicle (MAV) by the same descent bus; and limited capabilities for both surface mobility and payload manipulation to facilitate the buildup of a surface base.

Vehicle Design Evolution

The NTP vehicle concept presented here evolved directly from the archetypal concept reported in 1991[8] and shown in Fig. 1. System sizing supports the 2014 opposition mission with flyby abort; and hence, captures all Synthesis opposition and conjunction mission designs (subsequent NASA mission planning has come to emphasize all conjunction-class profiles, with opposition-return reserved for abort during the first 30 days at Mars). Differences in surface payload requirements for different mission staytimes are accommodated not by changing the transfer vehicle design, but by the number of robotic cargo transfer/lander missions sent ahead. Figure 2 shows the mission dates, Δv budget, transfer geometry, and optimized parking orbit specific to the 2014 opportunity, which together drive the system sizing discussed throughout this paper.

The new concept introduces several interesting and fundamental integration improvements: 1) a fully integrated structural spine in stackable sections; 2) a nontraditional, asymmetrical division and arrangement of main propellant tanks; 3) a microgravity transfer habitat module nestled within the forward ends of the main propellant tanks for radiation protection; and 4) engineering definition of all primary subsystems. Figure 3 shows the resulting configuration with key dimensions. Figure 4 tabulates system mass summaries for both expendable and reusable options; the configuration illustrated and discussed is the expendable baseline. Mass growth is included as indicated. Figure 5 shows an overall aft-starboard-quarter view.

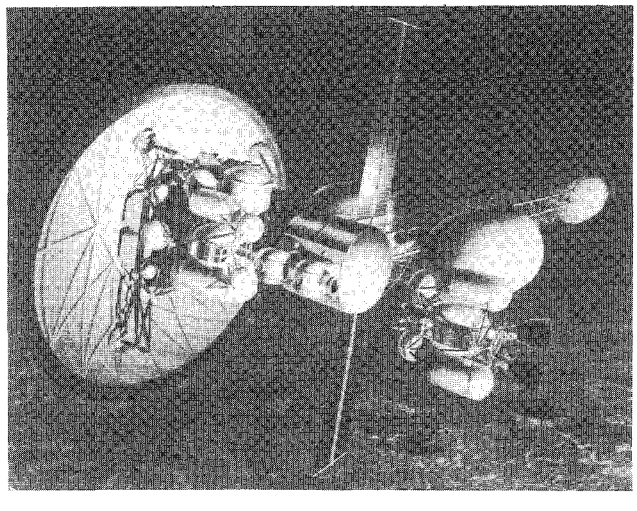

Fig. 1 Preliminary concept for Mars transfer vehicle using nuclear thermal propulsion (NTP).

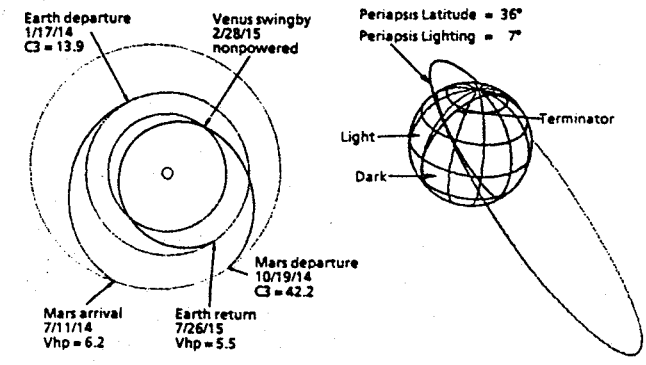

Δv (m/s)		Times (days)		Included losses (m/s)	
TMI	4490	Outbound time	175	TMI g-loss	300
MOC	3407	Mars staytime	100	TMI plane change	400
TEI	3840	Return time	290	MOI g-loss	50
Total	**11737**	**Total duration**	**565**		

Fig. 2 Optimized 2014 opposition mission parameters, trajectory, and parking orbit.

Propulsion System

Dual, advanced-NERVA-class NTP engines are baselined. Liquid hydrogen is the propellant. Propulsion system schematics, showing valves, manifolds, pumps, and so forth, are shown in Fig. 6. Boiloff, accumulated throughout the mission in spherical tanks located fore and aft (Figs. 5 and 7), is used both for attitude control (ACS) propellant and for pressurizing the in-line aft tank prior to the trans-Earth injection (TEI) and Earth orbit capture (EOC) burns. The three large drop tanks are pressurized during the TMI and Mars orbit capture (MOC) burns using hydrogen gas bled from the engine turbopumps, and for engine start by small, individual helium systems (visible in Fig. 7).

Traditional NTP configurations split the TMI and MOC hydrogen propellant, respectively, into two "strap-on" tanks each, positioned bilaterally symmetrically.[5] For the 2014 Δv breakdown, this would lead to significantly different gross tank sizes. A propellant–division trade for various tank diameters led to the asymmetrical configuration of three identical tanks shown: two lateral tanks (port and starboard) exclusively for TMI, and a dorsal tank for the remainder of TMI but primarily for MOC (about 90% of the tank volume). This leaves the ventral side of the vehicle free for lander integration as well as assembly and top-off access in LEO. It also limits the number of plumbing and other disconnects needed and allows a shorter overall vehicle. The tanks' identical size facilitates manufacturing and handling operations. The lateral tanks require only short-term passive thermal control provisions. The dorsal tank, which must keep hydrogen all the way to Mars, requires the same long-term storage technology as the aft tank (5 cm of multilayer insulation and vapor-cooled shields). Each 11.5-m-diam tank is sized for 5% ullage. An ETO launch capacity of 185 tonnes is appropriate if the three large tanks are launched fully wet.

The worst-case mass asymmetry during any mission phase requires only a 6-deg engine gimbal angle for compensation. High-torque (slow) electrohydrostatic actuators move each entire reactor/engine/nozzle assembly to achieve this. The lateral structure anchoring the actuators also supports the shadow shield. As shown, this shield is sized to prevent any scattered neutrons from reaching the forward part of the ship. It requires some simple deployment once launched ETO. Traditional options to reduce shield size (including lengthening the vehicle, repositioning the lander, and shaping the

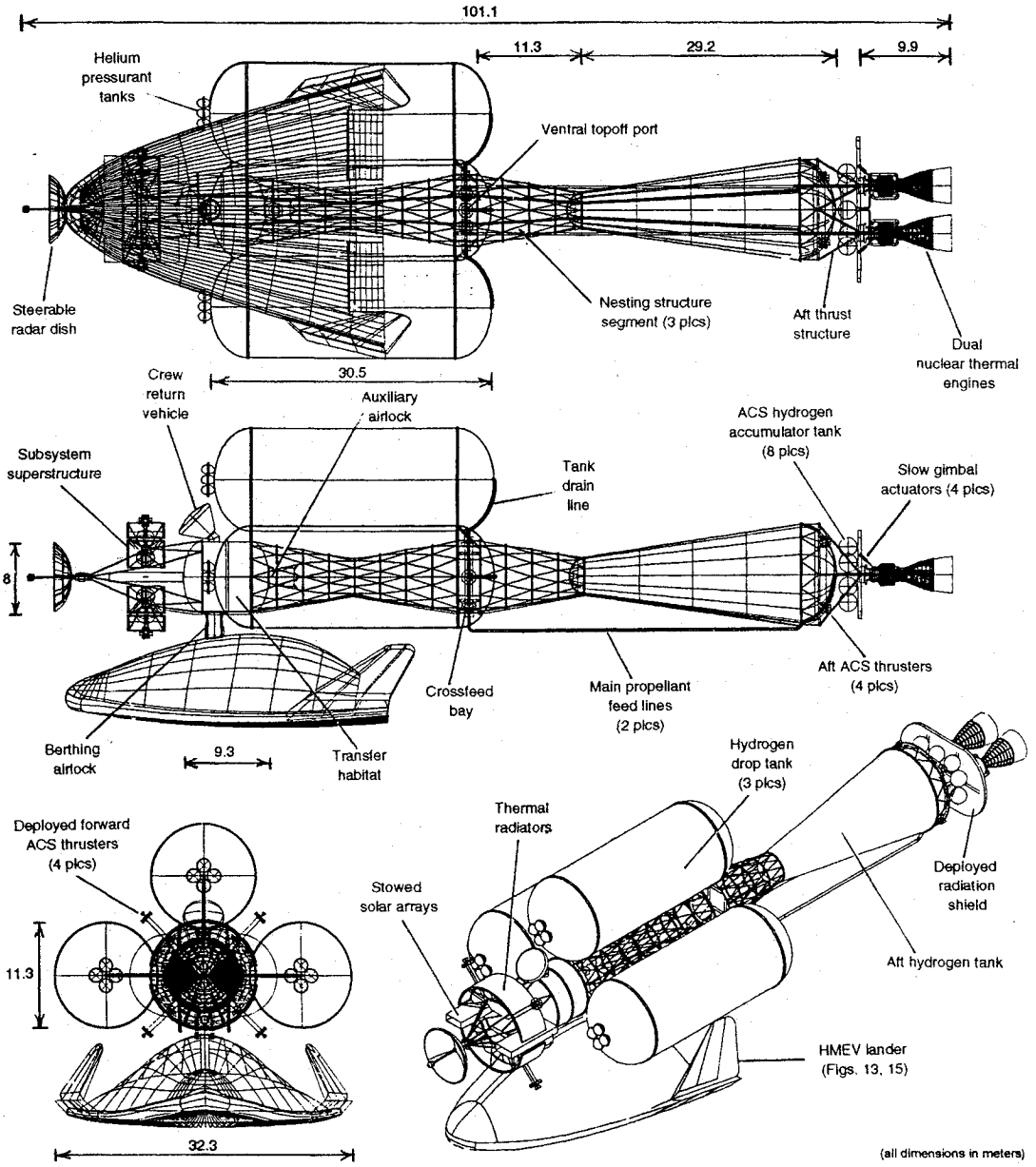

Fig. 3 Anatomy of integrated NTP vehicle concept.

aft ends of the hydrogen tanks) have only a small effect and trade poorly. Because no shield performance parametrics exist yet, shield geometry was not permitted to dominate other design drivers.

The propellant lines, hydrogen pressurization lines, and boil-off accumulation lines for the strap-on tanks are manifolded through valved quick-connects (QC) in a crossfeed bay amidships (Fig. 8). A propellant top-off port is also located here. Two redundant 12-in. stainless steel main propellant lines supply the aft manifold, bypassing the aft tank on the ventral side. Thermal contraction of these long propellant delivery lines during flowthrough is less than 15 cm, accommodated by dual bellows near the forward disconnects. The two main lines are installed in LEO. Perfect sealing of the field joints is not required because of the relatively short duration of hydrogen flowthrough.

Habitable Systems

The habitat is shown in Fig. 9. Made of a metal-matrix composite, it is a 7.6 × 9.2 m cylinder with ellipsoidal end domes, bisected by a pressure bulkhead for depressurization contingency. Specific volume is kept small by packaging the interior equipment for microgravity use. Crew quarters are located centrally, in the best-shielded region of the module, because the crew spends over a third of their time there. Functional areas are zoned by activity, and the "public" spaces for gathering, recreation, and exercise are located in the more spacious end domes.

The reference airlock is a two-crew-member, single-chamber design, 2 m in diameter and 2.5 m long, adapted from 1991 Freedom design data. "Equipment lock" functions, such as suit support, are incorporated into the parent habitat module. Berthing adapters at both ends allow modular integration and changeout, and an additional side hatch allows egress while both ends are berthed. Only one of the two mission airlocks is hyperbaric-capable.

The crew return vehicle (CRV) is an Apollo-style direct entry capsule sized for the mission crew of six (Fig. 10). Shown berthed to the top of the habitat module in Fig. 7, it separates from the returning NTP transfer vehicle just 12 h prior to Earth arrival, and performs a ~ 20 m/s maneuver to target the atmosphere (the transfer vehicle itself is on a trajectory that bypasses Earth).

Structure System

Limiting on-orbit assembly to comparatively simple operations results in a highly integrated approach to the main structure. The need for a long, stiff structure to package well for launch, be assembled easily in space, and support multiple fluid and electrical utilities was met with a new spine concept: three segments of conical, circular truss analogous to the metering optical benches used in the

Crew Systems Payload			60.5	
Habitat and internal subsystems		34.5		
Exterior power, TCS, communications		4.4		
Airlocks (2, 1 hyperbaric)		6.0		
Crew and consumables		14.3		
MMUs (2 + consumables)		0.8		
CRV			5.8	
HMEV (cryo descent, 6 crew, 9t cargo)			72.5	
Structures			5.5	
Attitude Control System			14.6	
Accumulator tanks		14.3		
Plumbing		0.3		
Hydrogen Plumbing			4.6	
Main lines		2.0		
Crossfeeds, valves, fittings		2.1		
Pressurization lines		0.5		
NTP Engines (2 @ T/W=10, Isp=925s)			6.8	
Radiation Shield System			6.8	
		Expendable		*Reusable*
Tankage and Propellant			639.6	851.0
Aft tank dry		15.0		27.0
Drop tanks dry (3)	2014 opposition, Venus swingby	77.1		96.9
EOC propellant		0		32.7
TEI propellant		73.2		98.6
MOC propellant		148.4		186.0
TMI propellant		325.9		409.8
Total IMLEO (metric tonnes)			817	1028

Fig. 4 Baseline concept mass summary.

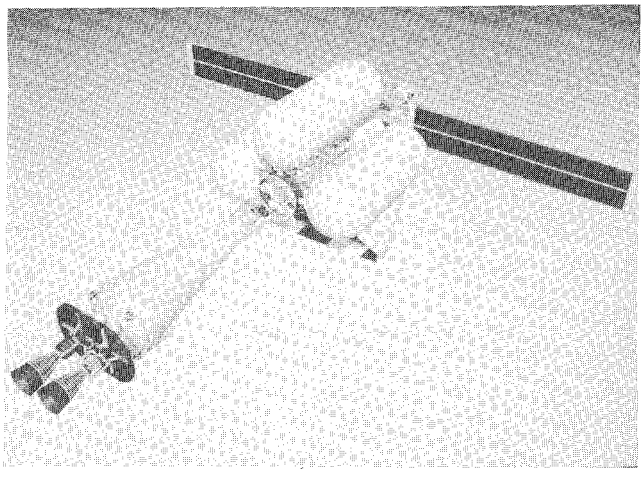

Fig. 5 Starboard aft-quarter view of engineering solid model.

Hubble and AXAF telescopes, made of a metal-matrix composite. Their diameter is 8 m at one end and 4 m at the other. These structure segments contain pre-integrated, redundant external conduits for power, data, and control lines; tank pressurization lines; and hydrogen boil-off accumulation lines. On-orbit assembly is reduced to a sequence of berthing operations. The structure segments, stowed for ETO launch like stacked Dixie-cups, are inverted and mated robotically. As the segments latch together, QC mechanisms at each end establish utility continuity.

The structure segments are each half as long as the barrel of the standard propellant tanks; structural attachment occurs at the tank shoulder-rings. Fluid disconnects between the drop tanks and the vehicle are located between the tanks' aft structural latches, an arrangement (analogous to the Shuttle external tank mounting) that assists QC alignment. The forward frustum of the aft tank matches the structure-segment half-angle, so that the aftmost segment can be stacked on top of the aft tank for launch inside the baselined 32-m-long shroud.

The transfer habitat module is oriented in line with the vehicle axis, allowing a simple structural interface to the forward segment of the circular-section main structure. This makes the forward shoulder rings of the three hydrogen drop tanks even with the aft shoulder ring of the habitat; this in turn nests the aft half of the module within the cluster of the forward ends of the tanks. Because the dorsal tank is virtually full of hydrogen for the outbound trip, this proximity

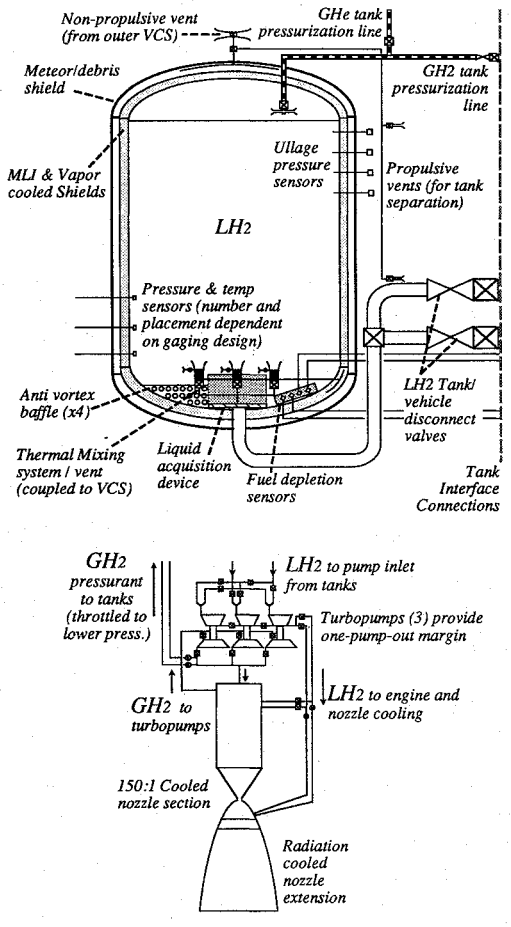

Fig. 6 Tank and main propulsion schematics.

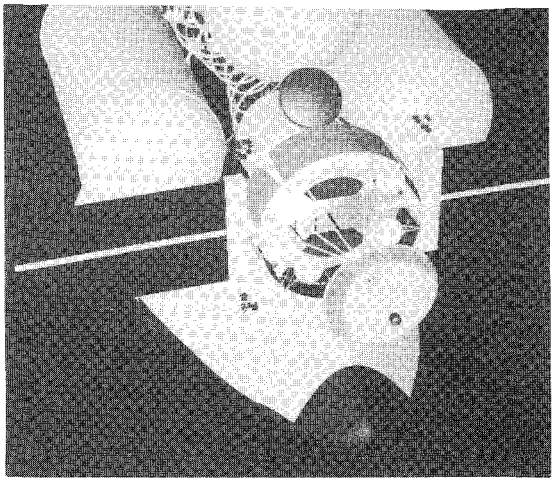

Fig. 7 Forward subsystems superstructure.

helps limit radiation fluence to the crew. The lateral tanks are retained, empty, until just prior to MOC to provide additional protective mass. Numerical radiation transport analysis using the CAD vehicle model reveals that the annual galactic cosmic ray dose inside the habitat module is within the 1989 NCRP limits recommended for (LEO) astronauts.

Furthermore, the galley region (rich in hydrogenous materials) provides a place within which the dose received from a benchmark solar flare (such as the 1959, 1972, or 1989 events) would be within the 1989 NCRP 30-day limit, even for the inbound mission leg.[10]

The in-line habitat orientation also allows simple integration (through an airlock) of the MAV crew cab, which is located just inside the top surface of the HMEV aerobrake. The HMEV is oriented parallel to the vehicle axis also, with wingtips folded to reduce its aspect from the shadow shield. A second airlock, accessible from

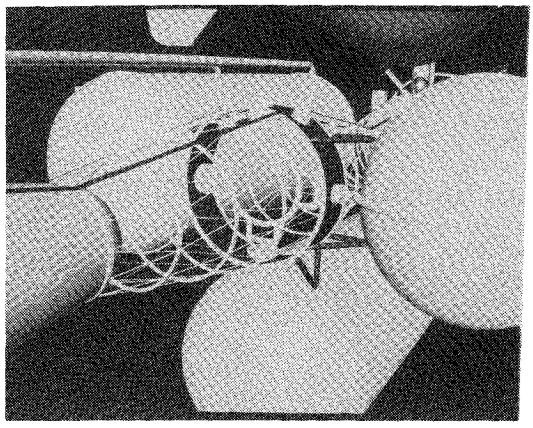

Fig. 8 Integrated structure system and crossfeed bay.

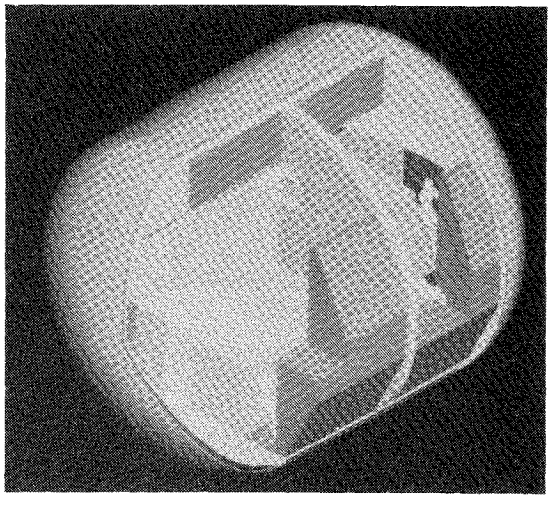

Fig. 9 Cutaway view of long-duration transfer habitat.

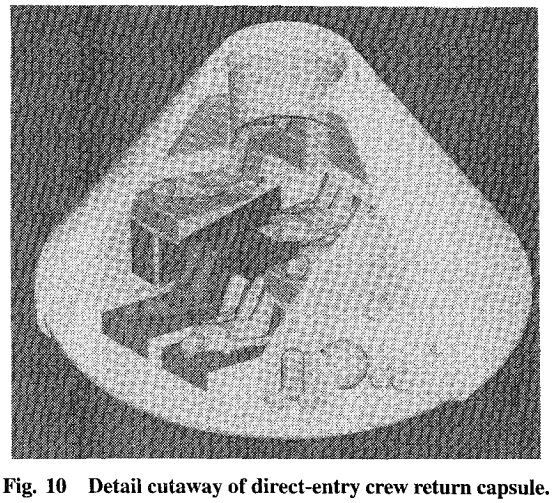

Fig. 10 Detail cutaway of direct-entry crew return capsule.

the aft pressure compartment of the transfer habitat, is located axially on the aft habitat end-dome, inside the forward structure segment. The strut spacing of the segments allows a suited astronaut passage to the exterior of the structure for extravehicular activity (EVA).

Utility Subsystems

A superstructure mounted to the forward shoulder-ring of the transfer habitat (Fig. 7) contains key subsystems: 1) a ring-shaped configuration of radiator heat pipes (120 m^2) for habitat and power system thermal rejection; 2) the forward ACS boil-off accumulator tanks, and redundant thrusters on extendible booms oriented to avoid plume impingement on the HMEV; 3) two extendible photovoltaic blankets (sized to produce 64 kWe peak at Mars), storage batteries for eclipse periods and engine burns, and power conditioning equipment; and 4) navigation equipment (star trackers, inertial and horizon sensors), communication equipment (7 m tracking high-gain dish and laser telescopes), and scientific instrumentation. Although partial solar array deployment is permissible within the radiation-shield shadow, full stowage is baselined for main propulsion maneuvers. The nominal orbital attitude in planetary space is head-down gravity-gradient stable, with the thermal radiator ring normal to planet nadir. The aft ACS subsystem also consists of eight accumulator tanks, attached directly to the radiation shield structure. Four nondeploying thruster modules, aligned with the forward thruster modules, are attached to the aft tank Y-ring within the 12-m-diam launch shroud envelope.

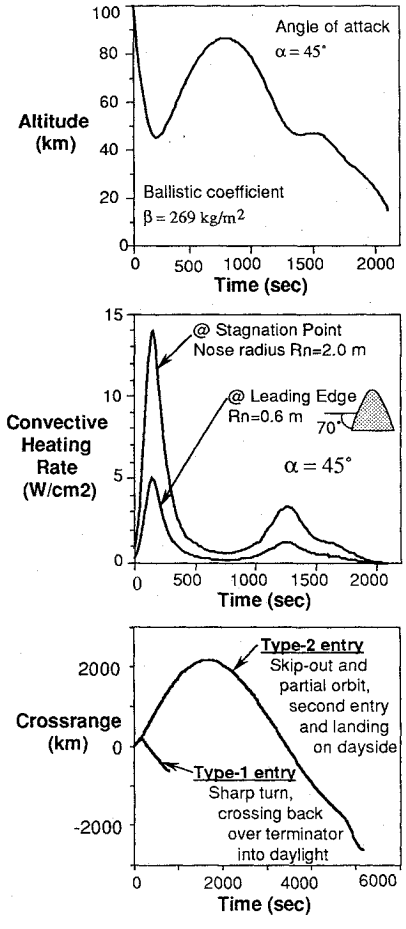

Fig. 11 Results of numerical descent simulations for the reference lander (HMEV), showing altitude history, thermal regime, and two methods of landing in daylight.

Launch and Assembly

Volumetrically, the NTP concept as shown could be packaged into just five ETO flights. The first launch would take the entire forward end: habitat, airlocks, and forward superstructure, fully integrated and stacked on top of the reversed, forward main structure segment, into which is nested the middle segment already integrated with the crossfeed bay. This core would have available all support subsystems (except ACS propellant) necessary for LEO operations. The HMEV (carried on the outside of this first ETO rocket, analogous to the Shuttle orbiter) could provide ACS capability once berthed. The second launch would consist of the entire aft end, with the aftmost main structure segment inverted and stacked on top. The two main propellant lines, brought by this launch also, would then be installed robotically. Three more launches would bring each of the three strap-on hydrogen tanks, fully wet. The CRV would come separately, boarding the crew prior to mission departure.

This manifesting concept, including mass allowances for removable LEO debris armor, payload support structure, and launch

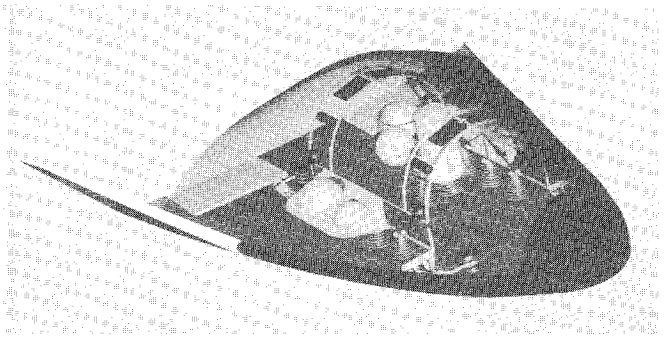

Fig. 12 Starboard forward-quarter view of HMEV engineering solid model.

HMEV Systems	Crew Version		Cargo Version	
MAV (ascent stage)				
Crew Cab	4250			
N2O4 (includes 3% steering loss)	17,281			
MMH (includes 3% steering loss)	9095		(no ascent stage)	
RCS Propellant	244			
Propellant Tanks	1567			
Propulsion Syst. (engines, lines, etc.)	649			
Structure	391			
Stage total	**33,477**			
Lander bus (descent stage)	**(Cryo)**	**(Storable)**	**(Cryo)**	**(Storable)**
Cargo	8904	5646	40,939	37,681
LH2 (MMH)	1709	5399	1709	5399
LO2 (N_2O_4)	10,252	10,259	10,252	10,259
RCS Propellant	1103	1087	1103	1087
Propellant Tanks	1969	1576	1969	1576
Propulsion Syst. (engines, lines, etc.)	1296	1296	1296	1296
Structure	1316	1316	1316	1316
Wheels	-----	-----	331	331
Drive Syst. (motors, susp., etc.)	-----	-----	675	675
Power Syst.(10 kWe arrays & batt.)	-----	-----	285	285
Landing Legs	817	817	-----	-----
Robotic Manipulator System	1000	1000	1000	1000
Aerobrake	10,644	10,644	11,612	11,612
Stage total	38,010	39,040	72,487	72,517
HMEV TOTAL (kg)	72,487	72,517	72,487	72,517

All values except cargo and propellant mass include 15 % growth

Fig. 13 HMEV mass summaries.

shroud, would require an ETO lift capacity of ~185 tonnes. The nonpropellant launches fully utilize the available 12 × 32 m shroud volume, including a 30-deg half-angle nose cone. Thus, the integrated NTP vehicle concept provides a datum for rigorously matching lift capacity to shroud size and setting both at an appropriate level for Mars exploration missions. For lift capacities less than 185 tons, a variety of approaches is available requiring six or more ETO flights and propellant topoff in LEO.

Reference Lander

A wide range of lander hypersonic L/D, from roughly 0.2 to over 2.5, has been analyzed for various kinds of Mars missions. STCAEM had already developed integrated vehicle concepts for Mars landers with $L/D = 0.5$ and $L/D = 1.1$.[8] The HMEV concept reported here as payload for the NTP transfer ship extends this integration experience to $L/D = 1.6$ for the following important reasons. Site selection for the 2014 initial mission is critical if landed assets are to be used for subsequent base buildup. But mass sensitivity for high-thrust (e.g. NTP) transfer propulsion causes the TEI vector to constrain the departure-orbit plane at Mars. Moreover, nodal regression, which could be used to precess the parking orbit to this required plane from an arrival orbit selected to admit a particular landing site latitude, is generally insufficient for this purpose given the short staytime at Mars afforded by opposition-class profiles. However, combining substantial cross-range capability on atmospheric entry with sufficient plane-change capability on ascent can significantly broaden the latitude band accessible from the parking orbit, even on the first mission. Thus higher L/D can be part of an overall strategy to enhance scientific payback despite the inherent limitations of high-thrust, opposition-profile mission designs.

$L/D = 1.6$ can maneuver from optimized parking orbits for all mission opportunities of interest (including the 2014 design case plotted in Fig. 2) to land in the daylit hemisphere anywhere within ±20 deg of the equator. $L/D = 1.6$ also provides improved control authority over lower L/D values. Although the need for this additional performance capability is not yet established, Mars' atmosphere is dramatically unpredictable, characterized by spatial density waves with amplitudes reaching ±50%. Finally, although higher L/D does induce higher heating, it does so over a significantly smaller surface area; thus the integrated vehicle design requires smaller amounts of heavy thermal protection. This effect is especially pronounced for trajectories suffering high radiative heating (e.g. direct-entry cases, such as for cargo delivery or other "direct" mission profiles). Because these four issues—site-selection; daylight landing; control authority; and thermal management—are key general drivers of Mars mission design, it is important to understand integrated lander vehicle design for $L/D = 1.6$. Figure 11 shows some descent performance characteristics of the selected shape[11]; actual design entry velocity is 4.85 km/s.

The HMEV can support either unmanned cargo delivery or crew-carrying missions (Fig. 12). It accommodates three different kinds

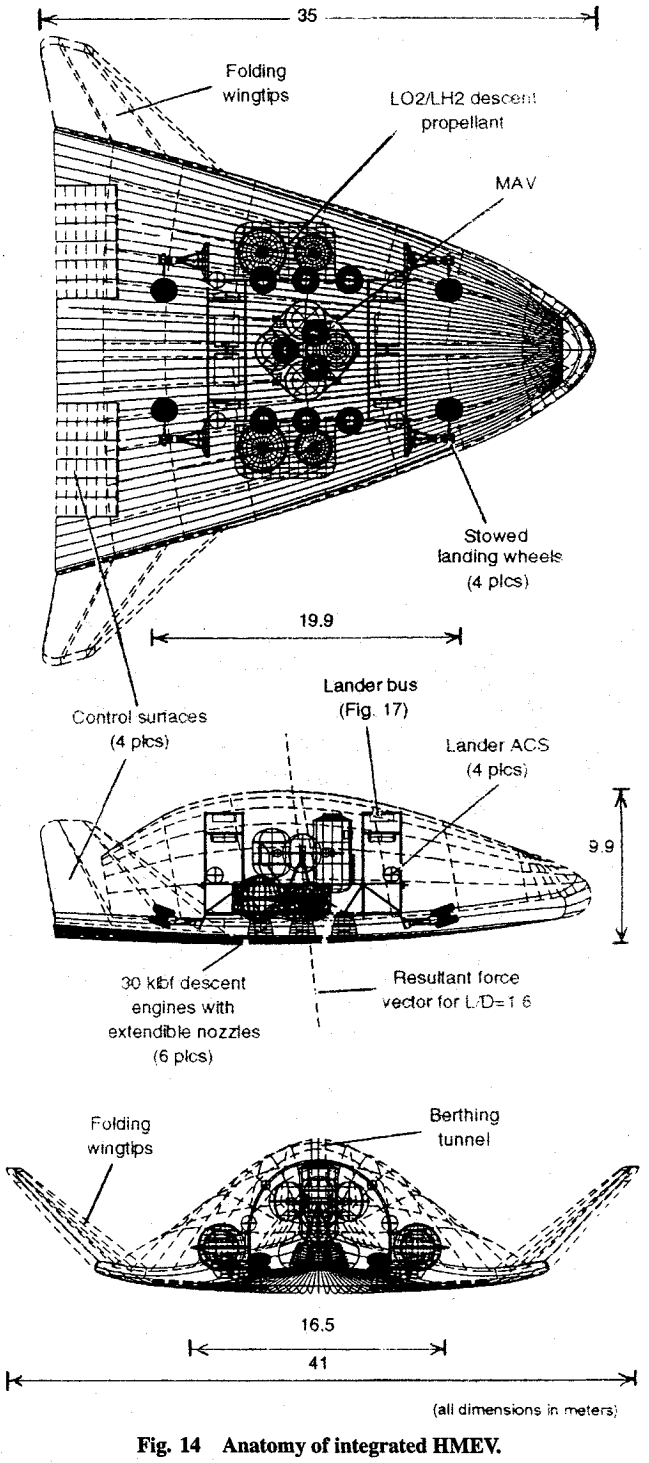

Fig. 14 Anatomy of integrated HMEV.

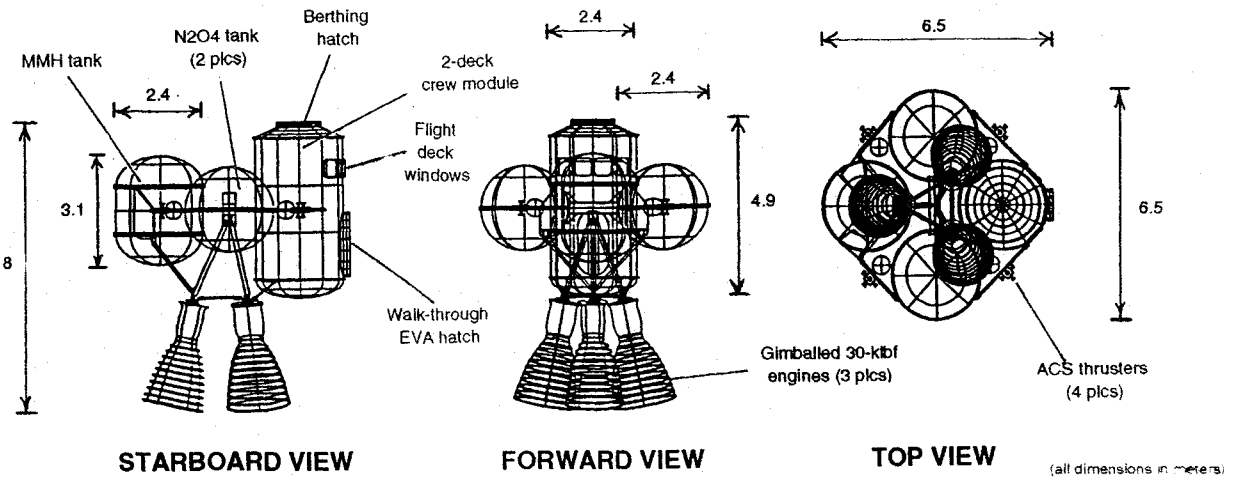

Fig. 15 Anatomy of crew-carrying ascent vehicle (MAV).

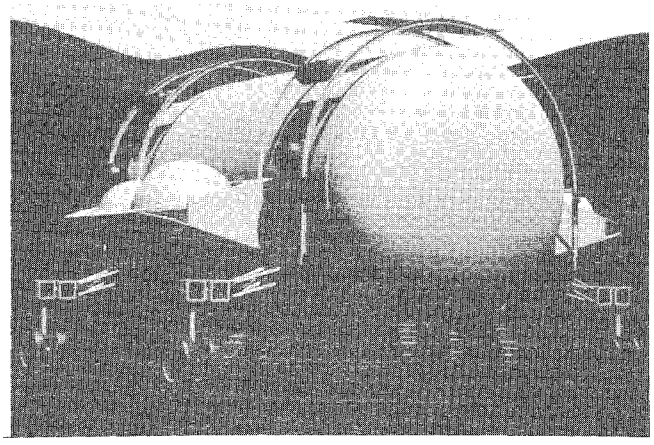

Fig. 16 Slow-roving lander concept.

of payload manifests: 1) bulky and heavy cargo, for example, an 8-m-diam long-duration surface habitat module sized for six crew members; 2) mixed cargo, for example, collections of rovers, science equipment, power systems and supplies; and 3) the ascent vehicle (MAV) for crew-carrying missions. It also solves in an integrated fashion two perennial problems: touchdown proximity for multiple landers, and cargo offloading and surface positioning.

The concept is expendable and staged, for minimal mass. The reference cargo version can deliver over 40 tonnes gross to the surface, whereas the reference crew version can deliver over 10 tonnes in addition to the complete MAV. Thus two HMEVs (one for crew and one sent ahead robotically for cargo) can support the 30-day reference mission surface stay; four (three cargo vehicles) would be required to support a 600-day-class conjunction stayover. Figure 13 tabulates mass summaries for both the cargo and crew-carrying versions, with cryogenic and storable descent-propellant options for each. Figure 14 shows configuration anatomy with key dimensions.

The aerobrake heat shield structure consists of cast C/Mg frames and ribs backing up a hot-structure surface of Ti/Al_3 honeycomb (face sheets bonded to a superplastically formed, laser-welded "egg crate" core). The approximately 30% of the heat shield requiring additional thermal protection is plasma-sprayed with zirconia. The upper shroud is a simple skin-stringer structure, also of C/Mg metal-matrix composite for high specific stiffness and high specific strength. Not substantially different in dimension from the Shuttle orbiter, the HMEV can be launched intact, attached to the outside of an ETO rocket.

The aerobrake is installed in five sections around the lander, two on top and three below. At about 10 km descent altitude at Mars, the descent engine nozzles extend through ports in the brake's heat shield and start. The upper shroud splits along its length and is jettisoned in a controlled manner by small solid rockets. At the point where propulsive penalty due to the weight of the heat shield exceeds its aerodrag benefit, the lower portion of the brake is detached in three pieces, then pushed away and dropped by the deploying landing gear. Descent abort is available at all times during descent, because the MAV (containing the crew cab) is positioned for simple separation out the top of the lander assemblage.

The MAV (Fig. 15) is arranged with a short stack for good packaging within the HMEV. The crew cab responds directly to two key drivers, volume and shape. Pressurized volume per crew member is 24 m^3. The vertically oriented, 2.5 m diam cylinder integrates well with excursion vehicle geometry; allows a two-deck arrangement analogous to the Shuttle with good touchdown visibility for the flight crew; and permits both a small hatch on top for berthing to the transfer vehicle airlock and a submarine-type door hatch for straightforward EVA egress on the surface (the entire cab is depressurized for surface egress).

For ascent, cryogenic propulsion has marginally superior performance even for conjunction-class surface stays, but it requires absolute integrity of vacuum jacketing in the Mars atmosphere for the entire surface stay. The minutes-to-hours warning for an abort-to-orbit incurred thereby is incompatible with multiday, pressurized-rover crew excursions away from the MAV. Thus, storable propellants, running three 30 klbf engines, are baselined for configuration sizing. A modest nominal engine cant allows fully tracking the vehicle center of mass with any engine out during any mission phase. The propellant budget reflected in Figs. 12–15 is specific to the 2014 reference mission, including the slight steering loss caused by the engine cant and launch from landing sites within ±20 deg of the equator.

The lander bus consists of side frames bridged by two pairs of structure arches, leaving a large opening in the top for MAV integration. Attitude control, power, communications, and payload hoisting subsystems are located in the spaces between each pair of arches, with propellant crossfeed, data and power lines running in the structure channels. Solar panels are stowed with their active surfaces protected during descent, and deployed once on the surface. The power system is sized to collect and store a modest amount of solar power (1.5 kW) throughout most of the Martian day, allowing a higher-power, short-duration expenditure (10 kW for about 45 min) to provide "creeping mobility" (7 cm/s) to the chassis. Using this thrifty method, distances on the order of a kilometer (anticipated to be within nominal touchdown accuracy) can be covered in just a few days (Fig. 16). Frame stiffness, provided during flight by the cargo assembly, is not a driver after cargo unloading because of the slow surface travel speed.

The descent propulsion system is split bilaterally, with three redundant 30 klbf engines (operating nominally at 50% throttle) located along each gunwale. A single, light-lifting manipulator system with dual end-arms, capable of reaching all vehicle subsystems and payloads, travels on a closed-loop track running along both gunwales and both inboard arches. Both tank/engine assemblies are

removed from the bus after touchdown using this manipulator system. The grounded lander bus then becomes a permanent part of the evolving Mars-basing infrastructure.

Conclusion

This work builds upon the first three generations of Mars mission vehicle concepts, using lessons learned from space-flight and technology-development programs and advanced computer-based analysis and integrated design methods, to yield deeper understanding. This fourth generation of Mars mission vehicle concepts is based on extensive performance analyses of trajectories, propulsion, and atmospheric flight, as well as detailed, iterative design focusing on subsystem integration, numerical radiation modeling, man-systems accommodation, launch manifesting, and orbital and flight operations practicality. The resulting lander concept is capable of supporting many kinds of surface missions anywhere on Mars. Moreover, the resulting transfer vehicle concept is capable of carrying any type of lander, supporting all SEI mission constraints, and serving as a new baseline for Mars mission planning. Together, these concepts, and the methods that produced them, establish a challenging standard for integration completeness in human planetary mission conceptual design.

Acknowledgments

The author is grateful to NASA for funding NAS8-37857, and indebted to the Boeing concept development team for their outstanding work and perseverance: M. Appleby, P. Buddington, S. Capps, M. Cupples, S. Doll, B. Donahue, C. R. Fowler, S. Ledoux, K. Luschei, J. McGhee, J. Nordwall, E. R. Tanner III, B. Wallace, and of course G. R. Woodcock.

References

[1]Von Braun, W., *The Mars Project*, Univ. of Illinois Press, Urbana, IL, 1991.

[2]Nance, J. C., "Nuclear-Pulse Propulsion-II," *Planetology and Space Mission Planning*, edited by E. M. Weyer, Vol. 140, Art. 1, Annals of NY Academy of Sciences, New York, 1966, p. 396.

[3]Sherwood, B., "System Complications of Modern Manned Mission Technologies," Second AIAA Conference on Solar System Exploration, Pasadena, CA, Aug. 1989.

[4]Anon., "Report of the 90 Day Study on Human Exploration of the Moon and Mars," NASA (unnumbered), 1989.

[5]Woodcock, G. R., "Space Transfer Concepts and Analysis for Exploration Missions, Phase One Final Report," Boeing Defense & Space Group D615-10030-2, Huntsville, AL, March 1991.

[6]"Report of the Advisory Committee on the Future of the U.S. Space Program," U.S. GPO (unnumbered), Washington, DC, 1990.

[7]"America at the Threshold: Report of the Synthesis Group on America's Space Exploration Initiative," U.S. GPO (unnumbered), Washington DC, 1991.

[8]Sherwood, B., "New Space Vehicle Archetypes for Human Planetary Missions," AIAA Paper 91-2335, June 1991.

[9]Sherwood, B., "Mars Basing," *Space 92: Engineering, Construction and Operations in Space*, Vol. 2, American Society of Civil Engineers, New York, 1992, pp. 1964–1975.

[10]Woodcock, G. R., "Space Transfer Concepts and Analysis for Exploration Missions, FY91 Final Report," Boeing Defense & Space Group D615-10045-2, Huntsville, AL, Dec. 1991.

[11]LeDoux, S. T., and Vas, I. E., "Aerothermodynamic Environments of Aerobraking Vehicles for Manned Mars Missions," AIAA Paper 91-2872, Aug. 1991.